



OPEN

# Differential Scanning Fluorimetry provides high throughput data on silk protein transitions.

SUBJECT AREAS:

BIOPHYSICAL METHODS  
BIOMATERIALS - PROTEINSReceived  
22 April 2014Accepted  
16 June 2014Published  
9 July 2014Correspondence and  
requests for materials  
should be addressed to  
F.V. (fritz.vollrath@  
zoo.ox.ac.uk)Fritz Vollrath<sup>1</sup>, Nick Hawkins<sup>1</sup>, David Porter<sup>1</sup>, Chris Holland<sup>1,2</sup> & Maxime Boulet-Audet<sup>1,3</sup><sup>1</sup>Department of Zoology, University of Oxford, South Parks Rd, Oxford OX1 3PS, <sup>2</sup>Department of Materials Science and Engineering, University of Sheffield, Mappin Street, Sheffield, S1 3JD, UK, <sup>3</sup>Department of Chemical Engineering and Department of Life Sciences, Imperial College London, South Kensington Campus, London.

Here we present a set of measurements using Differential Scanning Fluorimetry (DSF) as an inexpensive, high throughput screening method to investigate the folding of silk protein molecules as they abandon their first native melt conformation, dehydrate and denature into their final solid filament conformation. Our first data and analyses comparing silks from spiders, mulberry and wild silkworms as well as reconstituted 'silk' fibroin show that DSF can provide valuable insights into details of silk denaturation processes that might be active during spinning. We conclude that this technique and technology offers a powerful and novel tool to analyse silk protein transitions in detail by allowing many changes to the silk solutions to be tested rapidly with microliter scale sample sizes. Such transition mechanisms will lead to important generic insights into the folding patterns not only of silks but also of other fibrous protein (bio)polymers.

Differential Scanning Fluorimetry is a high throughput screening method for protein solutions using interactions of proteins with low-molecular-weight ligands<sup>1-3</sup>. Often also called the thermofluor assay or thermal shift assay, DSF is an inexpensive, simple and quick method that probes the refolding of a protein as it experiences progressive denaturation<sup>4,5</sup>. The technique relies on using specific dyes that fluoresce as they interact with proteins in their denaturation transition between a strongly hydrated solvated state and the final aggregated solid state. State-of-the-art quantitative polymerase chain reaction (qPCR) instruments can automatically process many controlled conditions and interactions in a single run and hundreds in a day<sup>1</sup>.

During a DSF experiment, denaturation is controlled by slowly heating the protein solution from a base-line, natural (i.e. stabilised and stabilising) temperature. This heating induces changes in the water shells and the hydrogen bonds, thus leading to associated adjustments in the conformation of the protein (Figure 1). Specifically designed dyes can interact with the bonds and signal this interaction by changes in their fluorescence spectrum. Here we present a set of measurements aimed to investigate the folding of silk protein molecules as they abandon their first native melt conformation, dehydrate and denature into their final solid filament conformation. We conclude that DSF provides a powerful tool to analyse silk protein transitions in depth and with the potential of generic insights also into the structures, properties and functions of silks and other fibrous proteins.

Such information on transitions is of fundamental importance for better understanding a protein's biochemistry, its structure-function relationships and its resistance to chemical, mechanical, and thermal denaturation<sup>6</sup>. Most diagnostic methods rely on the establishment of equilibrium between the folded and unfolded forms of a protein, and on an analysis of the ratio between the various states as conditions change and the protein slowly denatures in response. For example, optical techniques such as circular dichroism (CD)<sup>7-9</sup>, infrared spectroscopy (IR)<sup>10-12</sup> and dynamic light scattering (DLS)<sup>13</sup> are routinely used for studies of protein thermodynamics. Since the absorption of circularly polarized light is weak and decreases upon protein precipitation, this technique typically requires concentration higher than 1 mg/ml. For infrared spectroscopy, the strong absorption of water and its temperature dependency limits the applicability of technique for thermodynamic studies. Although sensitive to increasing radius of protein gyration during aggregation, DLS can be insensitive to unfolding mechanisms not affecting the size of the protein. In addition to optical techniques, the exo-endo-thermic probing of differential scanning calorimetry (DSC) has become a key tool to examine a protein's denaturation and glass transition temperature<sup>14-16</sup>. While providing valuable information, all these techniques can generally only thermally probe one sample at a time, which imposes severe limitations on screening studies or for analytical statistics.

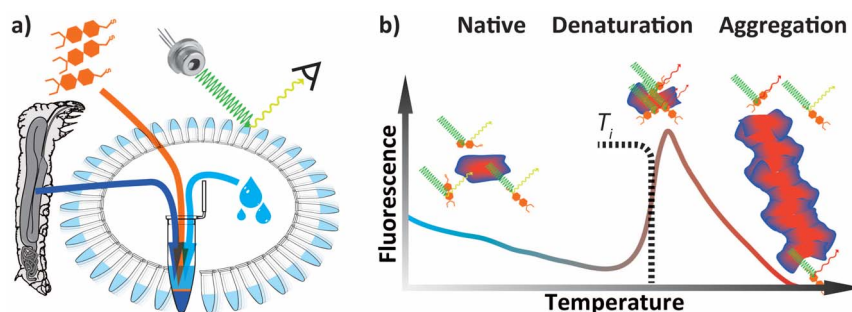


**Figure 1 | Differential Scanning Fluorimetry (DSF) aka ThermoFluor Assay aka Thermal Shift Assay technique and signal.** (a) Schematics illustrating the sample preparation for high throughput dynamic scanning fluorimetry thermal stability assay (b) Cartoon representing the native, denaturated and aggregated states of protein alongside its typical exogenous fluorescence response.

In contrast, fluorescence spectroscopy is extremely sensitive, often requiring less than parts per trillion for detection<sup>17</sup> and can ultimately detect a single molecule<sup>18</sup>. As we shall demonstrate, differential scanning fluorimetry (DSF) is a highly sensitive analysis tool that allows low protein concentrations to be probed at remarkable resolutions of temperature transitions. Importantly, the sample throughput using DSF can be substantial in multi-well thermal cycling machines, which have been perfected in the service of DNA screening analysis. Key to such DNA analysis is its amplification via the PCR technology, which uses temperature cycling in order to allow the controlled reaction of heat-sensitive polymerase enzymes. With the rapid expansion of DNA cloning, real-time PCR machines with accurate temperature control have become ever more affordable and are now wide spread tools. The high throughput enables the concurrent study of many experimental conditions, and it has for example been used to evaluate the stabilising effect of an array of ionic liquids on a common protein<sup>4</sup>.

In addition to its features of high throughput and low costs, DSF technology has led to the development of a wide variety of specific exogenous fluorescent molecules, which makes it an extremely versatile technique<sup>19</sup>. In a typical application, temperature transitions are used to probe the interactions of a protein with a fluorescent dye as it binds with specific sites such as residues exposed during unfolding<sup>20,21</sup>. Sypro® orange is well suited as dye of choice as it was designed specifically to activate fluorescence when binding to hydrophobic patches exposed as a result of conformational changes<sup>22</sup>. Using such a specific dye, DSF elicits and identifies key temperature transitions and protein stability features<sup>23</sup>, which in turn allows the probing and analysis of molecular interactions. Other dyes designed to bind to hydrophobic regions of amyloid fibrils<sup>24</sup> might also be of interest because silk and amyloid fibrils share important folding characteristics<sup>25</sup>. Moreover, highly specific antibodies with labels such as the green fluorescent protein (GFP) could also be used with DSF in order to target specific domains of a protein<sup>26,27</sup>.

Silk is a perfect model material for the study of protein denaturation. Firstly, Nature has evolved many thousands of silks, which between them sport many minor as well as major sequence differences<sup>28,29</sup> in addition to displaying key differences in processing (i.e. dehydration/denaturation) parameters<sup>30–32</sup>. Secondly, unlike most other proteins, silk proteins have evolved to denature ‘on demand’ in order to assume their 3<sup>rd</sup> functional ‘state’ i.e. that of a thread. A silk’s 1<sup>st</sup> state has the molecule in its long-term storage conformation. Its 2<sup>nd</sup> state occurs during the rapid structural reconfiguration during spinning. This three state transition progress is genetically pre-programmed, which makes silk protein conformation transitions interesting and valuable generic research tools. For example, there is overlap with amyloid formation<sup>33</sup> yet in the case of silks this is not an errant ‘mis’-folding pathway but the result of design by evolution. One could consider the 1<sup>st</sup> state to be classed as *active* (alive) - for the protein molecules stored in the gland are labile and easily denatured if

perturbed. The 2<sup>nd</sup> state could be called *re-active* - for each molecule refolds and reconfigures according to the environmental conditions it experiences in the controlled environment of the spinning duct. And the 3<sup>rd</sup> state could be deemed *inactive* (dead) - for the denatured protein molecules no longer respond actively as individuals to environmental conditions. Instead, they are now firmly locked into a polymer network, responding passively and collectively to stresses and strains imparted on the bulk material. Whether one agrees with this view or not, it is well established that silk molecules have two different states linked by a distinct, one-way transition<sup>34,35</sup>. We may assume that 400 M years of selective tweaking and tuning will have evolved a ‘spinning’ process that is highly advanced. The three major independent evolutionary pathways (in insects, arachnids and crustaceans<sup>36</sup>) that have led to more or less the same proteins and processes suggest to us that silks can provide insights into protein denaturation that are likely to be fundamental and of generic relevance.

## Results

Here we examine the transition from native to denatured in 3 specific silk protein complexes. We note that a silk typically consists of two distinct, different and large fibrous proteins (in the 3 cases presented here well characterised<sup>37,38</sup>) with some small molecules (mostly unknown and of unknown function<sup>39,40</sup>) in the mix. While the fibres of all three examples are inherently not very different when mechanically tested, the folding pathways, and thus the assembly mechanisms, clearly are distinct - as our DSF data demonstrate.

Convention assigns a protein a ‘melt’ temperature  $T_m$  to denote the onset of molecular reconfiguration during denaturation; this is potentially confusing with the concept of  $T_m$  in the polymer literature. To avoid misunderstanding we call the point at which fluorescence changes most rapidly  $T_i$  to denote the temperature induced instability of hydrogen interactions so fundamental to the protein ‘melt’ concept<sup>41</sup>.

Shortly after reaching the instability temperature,  $T_i$ , the rapid protein aggregation causes dye dissociation and an associated decrease of fluorescence<sup>4</sup>. Comparable to the analysis of DSC signals<sup>42</sup>, also in DSF the first derivative peak highlights these key transitions. Outlined in Fig. 2, these transitions vary between silks. In *Nephila edulis* dragline spider silk, the key transition occurred around 48°C and in *Bombyx mori* mulberry worm silk it occurred around 67°C. Confirmation on the irreversibility of the denaturation process in our silks was provided by re-runs of the samples after 24 hours in a refrigerator (Fig. 2). RSF (Reconstituted Silk Fibroin) feedstock/dopes lack any denaturation related fluorescence peak (Fig. 2); importantly this observation strongly supports the argument (based on rheology measurements) that RSF dopes ‘denature’ significantly differently from native silks<sup>31</sup>.

We assert that DSF is a powerful tool to assign silk and silk-derived bio-protein conversions and for this we need to demonstrate that the fluorescence signal does indeed occur only during a true transition.

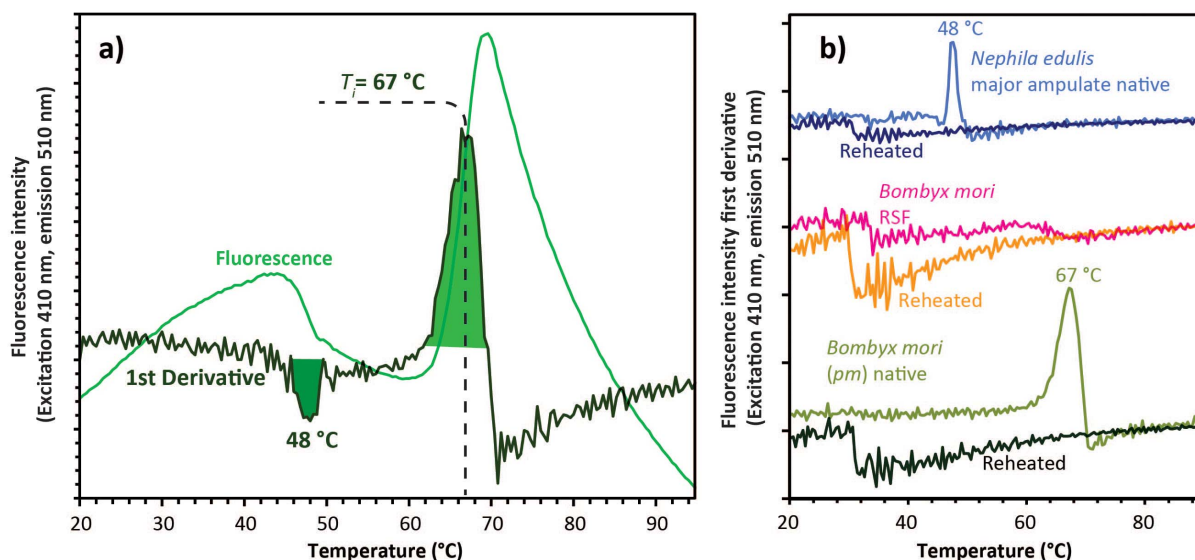


**Figure 2 | Temperature induced exogenous fluorescence response of Sypro® to the heating of native and denatured-reconstituted silk dope feedstocks.** (a) Representative fluorescence for *Bombyx mori* native silk dopes along first derivative response. (b) Comparative signals for spider, silkworm and reconstituted ‘silk’ (RSF) dope shown in the first derivative responses for *Nephila edulis* spider major ampullate silk, *Bombyx mori* mulberry silkworm native silk and a dope reconstituted from spun silk fibres (RSF). Responses of the materials were measured in a first run immediately shadowed by a second run (reheated), both following the same temperature ramps of 0.4°C/min increasing from 20 to 90°C using excitation of 470 nm and emission of 510 nm.

After all, irreversible denaturation, as outlined in the introduction, is supposed to be the key feature in the 3-stage active-to-inactive silk protein extrusion process of spinning a fibre from an aqueous dope. Our data (Fig. 2 and SM2) clearly demonstrate the irreversibility of the fluorescence signal on both spider and worm silks. Upon heating the sample a second time, the transitions observed at 48 and 67°C resp. completely disappear. The only remarkable feature that emerged during all repeating runs (i.e. reheating a dope a 2<sup>nd</sup> time) was a small drop i.e. decrease in fluorescence around 31°C, which we provisionally assign to a softening of the presumably gelled samples. Importantly, the DSF signal curve of the reconstituted silk feedstock (RSF) completely lacks any  $T_i$  peak at 67°C. Moreover, this material displayed rather similar responses to both the initial and the reheating runs with the small reheating drop at 31°C (Fig. 3), which suggests that the reconstituted silk prepared lacks the denaturation process of native dopes, be they from spider or worm silks. DSF thus corroborates previous rheology and scattering reports<sup>31,43,44</sup> and supports the theory that reconstituted silk lacks the molecular assembly behaviour characteristic of native silk dopes.

In comparison to the *Bombyx* dope, native dope from *Nephila edulis* major ampullate gland showed a weaker  $T_i$ , at the much lower temperature of 48°C. This feature could be explained by either (i) a smaller fraction of the protein undergoing denaturation or (ii) the spider silks having a much greater thermal instability<sup>45</sup>. Or indeed (iii) the spider silk dopes might have been at much lower concentrations, which was difficult to assess in this study due to a combination of small gland sizes and the variability in concentrations (C. Dicko personal communication). Fortunately we were able to source wild silk worms *Antheraea pernyi* that have silks with proteins more alike to spider silks than *Bombyx* silks despite a much closer taxonomic relationship with the latter<sup>46</sup>. So, to evaluate the effect of protein conformation and concentration on the  $T_i$ , we compared native silk dopes of *Bombyx mori* and *Antheraea pernyi*, which had been diluted in different ratios to provide dopes of specific concentrations. Importantly, the *Antheraea* wild silk dopes behaved much more like the spider silks dopes, although here we could also examine the effect of concentration.

Firstly, the overall signal pattern of *Antheraea* dope resembled the pattern of *Nephila* dragline dope (see SM3). Secondly, Fig. 3a shows

that the concentration affected strongly the signal integrated intensity for all native silk dope measured. Hence, it stresses the need for determining the sample concentration in order to compare intensity values. Figure 3b shows that the temperature trigger for both parts of the *Bombyx mori* silk gland is only weakly influenced by the protein. In contrast, the  $T_i$  of *A. pernyi* dope is much more dependent on the concentration whilst being at significantly lower temperatures.

Last but not least, we examined the effect of compounds known to stabilise molecules under hydration stress. After all, the study aimed to examine dehydration, and we hypothesised that a cryo/denaturation protectant such as trehalose<sup>47</sup> should have a measureable effect. Indeed, this turned out to be the case by decreasing the transition integrated intensity (Fig. 3c) and significantly shifting the folding temperature (Fig. 3d). This experiment demonstrates that trehalose somehow shields the bonds and thus manages to protect the folding conformation. As importantly for the concept, it demonstrates that DSF can indeed be used also to test compounds that might affect folding parameters in one way or another.

## Discussion

Our data demonstrate that DSF is a very powerful technique for detailed observations of clearly defined denaturation transitions in silks (Fig. 4). Not only were the quantitatively measured transitions highly specific for each of the silks tested, they also showed significant concentration dependences, which in themselves reveal underlying molecular folding differences between these silks. The signature of mulberry silk was significantly different from that of wild silk, which in turn was rather close to that of spider silk. The universal cryoprotectant trehalose shifted the folding signature slightly but significantly, thus demonstrating its shielding action. Last but not least, the technology clearly showed that reconstituted silks showed a folding pattern comparable to that of its denatured progenitor, which has important implications for the argument that RSF is not a silk *sensu stricto* and should neither be treated - nor called - as such<sup>48</sup>.

DSF also now allows us to formulate specific and testable hypotheses. For example, the  $T_i$  of folding transitions was relatively independent of dope concentrations in silks of *Bombyx mori*, which may suggest that 6000 yrs of farming for spinning consistency may have bred out any ancestral responses to dehydration stresses. Wild silk-

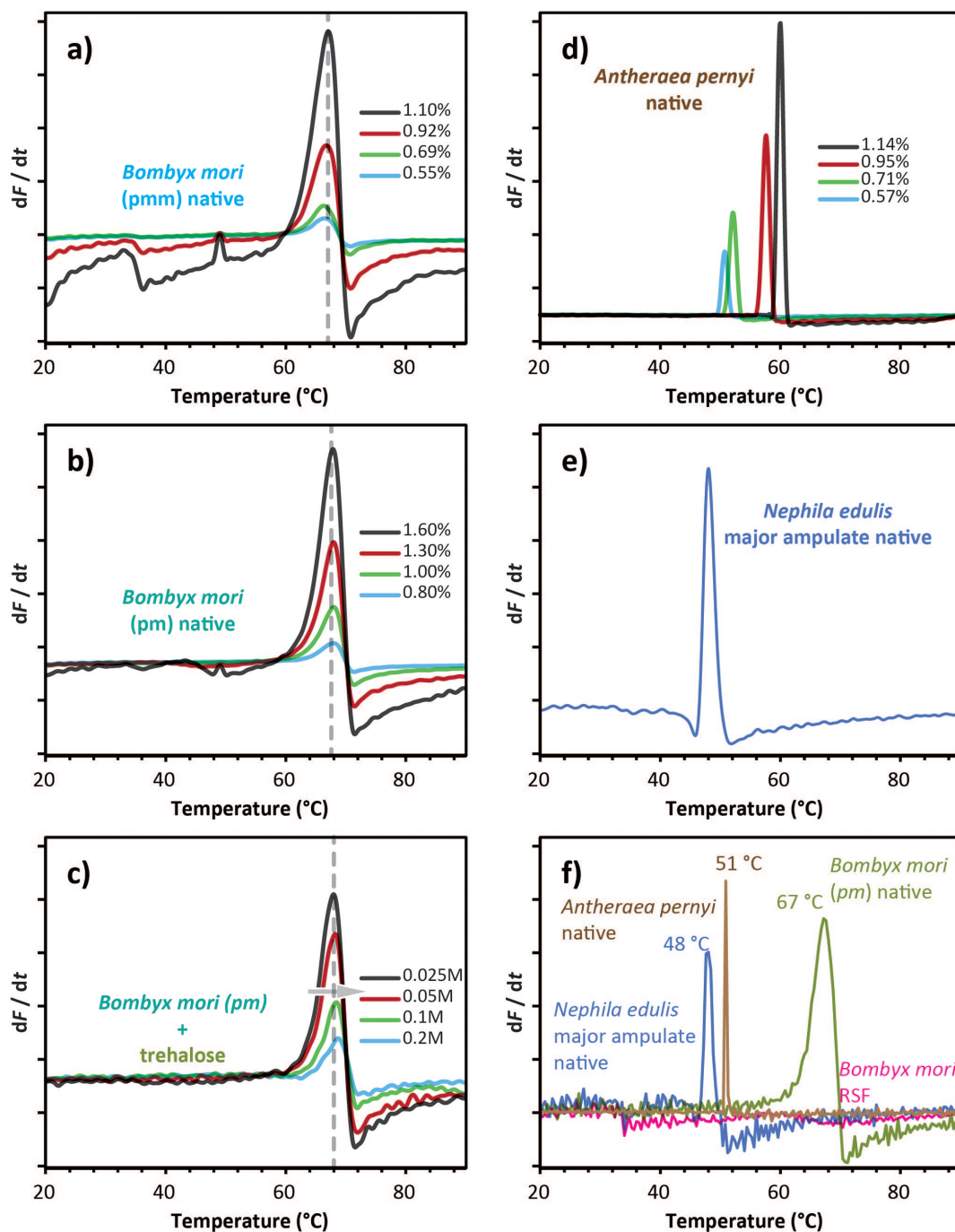


**Figure 3** | DSF fluorescence signals of various silks feedstock/dopes and dope concentrations. (a, b) For the ‘domesticated’ silk of *Bombyx mori* the signal decreases in strength as a function of silk dope concentration for two distinct major parts of the gland (pmm for middle section and pm for posterior section, details in SM). (c) For the ‘wild’ silk of *Antheraea pernyi* the picture is rather different with the signal shifting not only changing in strength but also shifting along the temperature ramp as a function of dope concentration. (d) The signals for dope from the Major Ampullate gland of the *Nephila edulis* spider resemble those for *Antheraea* dopes at high concentration. (e) Trehalose affects the signal of *Bombyx* dope (shown by the arrow) dependent on the concentration of the additive. (f) Overlay of the exogenous fluorescence intensity first derivative for native dope of *Bombyx*, *Nephila* and *Antheraea* as well as for reconstituted silk dope made using *Bombyx* silk fibres.

worms like *Antheraea pernyi* and spiders like *Nephila edulis*, on the other hand still live in natural habitats where desiccation is a real threat<sup>49</sup> and their silks have built-in mechanisms to shield against this. However this may be, the technique discussed here will allow us to draw possible and testable conclusions that relate not only to molecular mechanisms but also to evolutionary drivers behind them by using clade comparisons<sup>50</sup>.

Our first experiments with DSF reveals the power of this technique to quantitatively probe the underlying dynamics of a protein and

protein mix with the view of identifying patterns and perhaps even assigning activity patterns. Hypothesising on such assignments is not the purpose of this article introducing a tool novel to silk studies. Hence here we simply propose that DSF provides a powerful tool to screen for specific denaturation transitions. We assert that operating this tool will have significant implications for the ‘prospecting’ not only of silks but also of other natural bio-polymer proteins as well as for iterative testing procedures of synthetic or semi-synthetic ‘designer’ proteins.

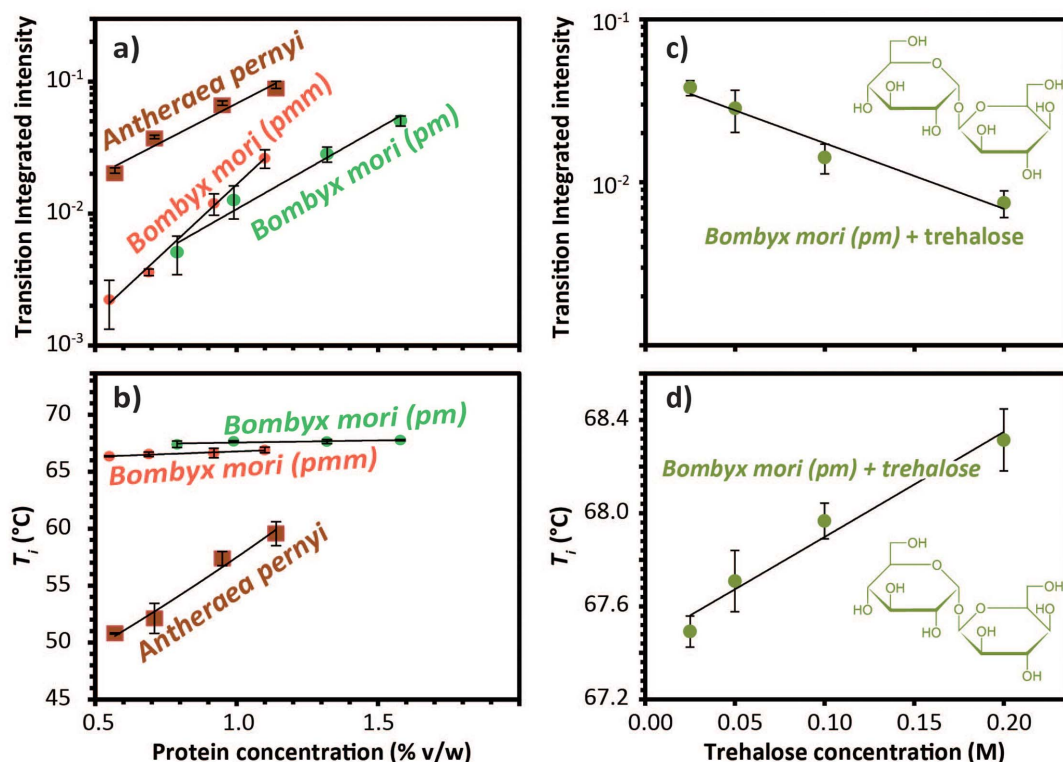


**Figure 4** | Analysis of DSF Data shown in Figure 3. (a) Integrated transition intensity as a function of the protein concentration for *Antheraea pernyi* and *Bombyx mori* posterior (pm) and middle (pmm). (b)  $T_1$  as a function of the protein concentration for *Antheraea* and *Bombyx* posterior (pm) and middle (pmm) sections. (c) Integrated transition intensity as a function of trehalose concentration for *B. mori* posterior section (pm). (d)  $T_1$  as a function of the trehalose concentration for *B. mori* posterior section (pm).

## Methods

Preparation of the silk samples is explained in detail in the supplementary methods SM1. In essence, the samples were either obtained (i) by dissection of the gland and by subsequent washing out of the silk-dope in Ringer's solution or (ii) by following traditional recipes to make reconstituted silk dopes RSF. After silk dope preparation, various amount of Sypro® Orange Merocyanine dye (Sigma Aldrich) were added to the silk solution<sup>19</sup> with the exception of control runs. Sypro® Orange has an absorption maxima at 470 nm and an emission maxima at 569 nm<sup>50</sup>. This dye was designed to have a weak intrinsic fluorescence but a strong fluorescence upon binding to protein (~500 fold). To homogenise the dyed solutions, samples were then protected from light and placed onto an orbital shaker at 60 rpm in a cold room at 5 °C for 9 to 16 hours. Sample concentrations (w/v) were determined by drying 200  $\mu$ L of sample on aluminium foil at 60 °C overnight and measuring the residual dry weight.

For the testing of the interactions between the dope and the dye, we deployed a Rotor-Gene Q (Qiagen, Venlo, Netherlands) originally developed for qPCR reactions. This instrument offers highly controlled, steady temperature ramps as well as high fluorescence sensitivity. The fluorescence signal was measured for 36 samples simultaneously using 5 independent channels (green, yellow, orange, red and crimson) respectively exciting at 470, 530, 585, 625 and 680 nm and emitting at 510, 557, 610, 660 and 715 nm. The green channel (excitation at 470 nm, emission at 510 nm) was not the most sensitive (which was yellow) but green offered the best dynamic range for probing the fluorescence of Sypro® orange interacting with silk protein over the concentration range studied (see Supplementary Methods). Fluorescence was measured continuously at 1 Hz (i.e. one data point per minute per sample) while temperature was gradually raised at 0.4 °C/min with the instrument spinning samples at 400 rpm, which ensures excellent mixing without causing phase separation. Gain was optimized at the beginning of each sample run and the resulting gain value was used to compare between runs; moreover, gain optimization provided the desired range of starting fluorescence at the start temperature for all channels. The standard deviations for each sample set were calculated from 4 repeats. We used the centre of gravity of the first derivative peak of the measurements in order to assure best accuracy for each calculation of instability transition temperature ( $T_1$ ). All results for each sample set were obtained within a few hours of each other.

Sypro Orange® was developed and indeed has become is the dye of choice for detecting most protein re-folding studies<sup>19,51</sup>. It also provided by far the best results also for our silks when compared to a number of other candidate dyes such as Nile Red, Congo Red and Rhodamine B, all of which are known or suspected to indicate molecular folding of silk proteins. Sypro Orange® is part of the merocyanine dye group, which change colour with changing polarity of the solvent<sup>52</sup>. Such solvatochromism occurs when the hydrophobic dye binds to our protein's hydrophobic domains<sup>53</sup>. In addition, the sulfonate function ( $-SO_3^-$ ) is likely to bind with buried

charged residues such as arginine<sup>54</sup>. Figure 2 shows the evolution of green fluorescence (i.e. measured by the green channel) in response to increasing temperature. Denaturation starts around 60 °C when water molecules progressively leave the protein backbone; this allows the dihedral angles around the amide bonds to rotate freely, which in turn leads to the adoption of progressively more stable conformations<sup>55</sup>. During this process the evolving configurations allow dye molecules to bind to hydrophobic patches as they expose themselves on the proteins surface<sup>4</sup>. Such binding delocalises the dye's electron, which substantially enhances fluorescence, in the case of Sypro® orange by more than 500 fold<sup>19</sup> making this dye's fluorescence a superb indicator of temperature induced protein denaturation process and product.

- Garner, H. R., Armstrong, B. & Lininger, D. M. HIGH-THROUGHPUT PCR. *Biotechniques* **14**, 112–115 (1993).
- Pantoliano, M. W. *et al.* High-density miniaturized thermal shift assays as a general strategy for drug discovery. *J. Biomol. Screen.* **6**, 429–440, doi:10.1089/108705701753364922 (2001).
- Matulis, D., Kranz, J. K., Salemme, F. R. & Todd, M. J. Thermodynamic stability of carbonic anhydrase: Measurements of binding affinity and stoichiometry using ThermoFluor. *Biochem.* **44**, 5258–5266, doi:10.1021/bi048135v (2005).
- Rodrigues, J. V., Prosiński, V., Marrucho, I., Rebelo, L. P. N. & Gomes, C. M. Protein stability in an ionic liquid milieu: on the use of differential scanning fluorimetry. *Phys. Chem. Chem. Phys.* **13**, 13614–13616, doi:10.1039/c1cp21187k (2011).
- Fan, Y. C. *et al.* Fluorescence Spectroscopic Analysis of the Interaction of Papain with Ionic Liquids. *Appl. Biochem. Biotechnol.* **168**, 592–603, doi:10.1007/s12010-012-9801-x (2012).
- Wright, N. T. & Humphrey, J. D. Denaturation of collagen via heating: An irreversible rate process. *Annu. Rev. Biomed. Eng.* **4**, 109–128, doi:10.1146/annurev.bieng.4.101001.131546 (2002).
- Arakawa, T. & Tsumoto, K. The effects of arginine on refolding of aggregated proteins: not facilitate refolding, but suppress aggregation. *Biochem. Biophys. Res. Commun.* **304**, 148–152, doi:10.1016/s0006-291x(03)00578-3 (2003).
- Safar, J., Roller, P. P., Gajdusek, D. C. & Gibbs, C. J. Thermal-stability and conformational transitions of scrapie amyloid (prion) protein correlate with infectivity. *Protein Sci.* **2**, 2206–2216 (1993).
- Greenfield, N. J. Using circular dichroism collected as a function of temperature to determine the thermodynamics of protein unfolding and binding interactions. *Nat. Protoc.* **1**, 2527–2535, doi:10.1038/nprot.2006.204 (2006).



10. Smeller, L., Rubens, P. & Heremans, K. Pressure effect on the temperature-induced unfolding and tendency to aggregate of myoglobin. *Biochem.* **38**, 3816–3820, doi:10.1021/bi981693n (1999).
11. Williams, S. *et al.* Fast events in protein folding: Helix melting and formation in a small peptide. *Biochem.* **35**, 691–697, doi:10.1021/bi952217p (1996).
12. Yan, Y. B., Zhang, J., He, H. W. & Zhou, H. M. Oligomerization and aggregation of bovine pancreatic ribonuclease A: Characteristic events observed by FTIR spectroscopy. *Biophys. J.* **90**, 2525–2533, doi:10.1529/biophysj.105.071530 (2006).
13. Nobbmann, U. *et al.* Dynamic light scattering as a relative tool for assessing the molecular integrity and stability of monoclonal antibodies. *Biotechnol. Gen. Eng. Rev.* **24**, 117–128 (2007).
14. Bruylants, G., Wouters, J. & Michaux, C. Differential scanning calorimetry in life science: Thermodynamics, stability, molecular recognition and application in drug design. *Curr. Med. Chem.* **12**, 2011–2020, doi:10.2174/0929867054546564 (2005).
15. Privalov, P. L. Intermediate states in protein folding. *J. Mol. Biol.* **258**, 707–725, doi:10.1006/jmbi.1996.0280 (1996).
16. Ahrer, K., Buchacher, A., Iberer, G. & Jungbauer, A. Thermodynamic stability and formation of aggregates of human immunoglobulin G characterised by differential scanning calorimetry and dynamic light scattering. *J. Biochem. Biophys. Methods* **66**, 73–86, doi:10.1016/j.jbbm.2005.12.003 (2006).
17. Richardson, J. H. & Ando, M. E. Sub-part-per-trillion detection of polycyclic aromatic-hydrocarbons by laser-induced molecular fluorescence. *Anal. Chem.* **49**, 955–959, doi:10.1021/ac50015a021 (1977).
18. García-Parajo, M. F., Segers-Nolten, G. M. J., Veerman, J.-A., Greve, J. & van Hulst, N. F. Real-time light-driven dynamics of the fluorescence emission in single green fluorescent protein molecules. *Proc. Natl. Acad. Sci.* **97**, 7237–7242, doi:10.1073/pnas.97.13.7237 (2000).
19. Haugland, R. P., Jones, L. J., Singer, V. L. & Steinberg, T. H. Molecular Probes, Inc., European patent, EP 0774122 A1, Merocyanine dye protein stains. 1997 May 21.
20. Vaiana, A. C. *et al.* Fluorescence quenching of dyes by tryptophan: Interactions at atomic detail from combination of experiment and computer simulation. *J. Am. Chem. Soc.* **125**, 14564–14572, doi:10.1021/ja036082j (2003).
21. Sonoda, Y. *et al.* Benchmarking Membrane Protein Detergent Stability for Improving Throughput of High-Resolution X-ray Structures. *Structure* **19**, 17–25, doi:10.1016/j.str.2010.12.001 (2011).
22. Niesen, F. H., Berglund, H. & Vedadi, M. The use of differential scanning fluorimetry to detect ligand interactions that promote protein stability. *Nat. Protoc.* **2**, 2212–2221, doi:10.1038/nprot.2007.321 (2007).
23. Vedadi, M. *et al.* Chemical screening methods to identify ligands that promote protein stability, protein crystallization, and structure determination. *Proc. Natl. Acad. Sci.* **103**, 15835–15840, doi:10.1073/pnas.0605224103 (2006).
24. Nilsson, K. P. R. Small organic probes as amyloid specific ligands - Past and recent molecular scaffolds. *FEBS Lett.* **583**, 2593–2599, doi:10.1016/j.febslet.2009.04.016 (2009).
25. Dicko, C., Porter, D. & Vollrath, F. The relevance of silks to amyloids. in *Functional Amyloid Aggregation*. Rigacci, S. & and Monica Bucciantini, M. (eds) 51–70 (Research Signpost/Transworld Research Network 2010) ISBN: 978-81-308-0425-5.
26. Moreau, M. J. J. *et al.* Rapid determination of protein stability and ligand binding by differential scanning fluorimetry of GFP-tagged proteins. *Rsc Adv* **2**, 11892–11900, doi:10.1039/C2ra22368f (2012).
27. Moreau, M. J. J. & Schaeffer, P. M. Dissecting the salt dependence of the Tus-Ter protein-DNA complexes by high-throughput differential scanning fluorimetry of a GFP-tagged Tus. *Mol. Biosys.* **9**, 3146–3154, doi:10.1039/C3mb70426b (2013).
28. Hayashi, C. Y. & Lewis, R. V. Molecular architecture and evolution of a modular spider silk protein gene. *Science* **287**, 1477–1479 (2000).
29. Sutherland, T. D. *et al.* An independently evolved Dipteran silk with features common to Lepidopteran silks. *Insect Biochem. Mol. Biol.* **37**, 1036–1043, doi:10.1016/j.ibmb.2007.05.016 (2007).
30. Vollrath, F. & Knight, D. P. Liquid crystalline spinning of spider silk. *Nature* **410**, 541–548 (2001).
31. Holland, C., Terry, A. E., Porter, D. & Vollrath, F. Natural and unnatural silks. *Polymer* **48**, 3388–3392 (2007).
32. Holland, C., Terry, A. E., Porter, D. & Vollrath, F. Comparing the rheology of native spider and silkworm spinning dope. *Nat. Mater.* **5**, 870–874, doi:10.1038/nmat1762 (2006).
33. Dicko, C., Kenney, J. M. & Vollrath, F. Beta-Silks: Enhancing and controlling aggregation. *Adv. Protein Chem.* **73**, 17–53 (2006).
34. Lucas, F. & Rudall, K. Extracellular fibrous proteins: The silks. *Compr. Biochem.* **26 Part B**, 475–558 (1968).
35. Knight, D. P., Knight, M. M. & Vollrath, F. Beta transition and stress-induced phase separation in the spinning of spider dragline silk. *Int. J. Biol. Macromol.* **27**, 205–210 (2000).
36. Craig, C. Evolution of arthropod silks. *Annu. Rev. Entomol.* **42**, 231–267 (1997).
37. Tamura, T., Inoue, H. & Suzuki, Y. The fibroin genes of *Antheraea yamamai* and *Bombyx mori* are different in their core regions but reveal a striking sequence similarity in their 5' ends and 5' flanking regions. *Mol. Gen. Genet.* **207**, 189–195 (1987).
38. Jackson, C. & O'Brian, J. P. Molecular weight distribution of *Nephila clavipes* dragline silk. *Macromol.* **28**, 5975–5977 (1995).
39. Zhang, P. *et al.* Proteome analysis of silk gland proteins from the silkworm, *Bombyx mori*. *Proteomics* **6**, 2586–2599 (2006).
40. Weiskopf, A., Senecal, K., Vouros, P., Kaplan, D. & Mello, C. M. The carbohydrate composition of spider silk: *Nephila edulis* dragline. *Glycobiol.* **6**, 1703 (1996).
41. Porter, D. & Vollrath, F. Water mediated proton hopping empowers proteins. *Softmatter* **9**, 643–646 doi:10.1039/C2SM27155A (2013).
42. Zhang, H., Takenaka, M. & Isobe, S. DSC and electrophoretic studies on soymilk protein denaturation. *J. of Therm. Anal. Calorimet.* **75**, 719–726, doi:10.1023/b:jtan.0000027168.18317.78 (2004).
43. Boulet-Audet, M., Terry, A. E., Vollrath, F. & Holland, C. Silk protein aggregation kinetics revealed by Rheo-IR. *Acta Biomater.* **10**, 776–784, doi:10.1016/j.actbio.2013.10.032 (2013).
44. Greving, I., Dicko, C., Terry, A., Callow, P. & Vollrath, F. Small angle neutron scattering of native and reconstituted silk fibroin. *Soft Matter* **6**, 4389–4395, doi:10.1039/c0sm00108b (2010).
45. Dicko, C., Porter, D., Bond, J., Kenney, J. M. & Vollrath, F. Structural disorder in silk proteins reveals the emergence of elastomericity. *Biomacromol.* **9**, 216–221, doi:10.1021/bm701069y (2008).
46. Zhang, Y., Yang, H., Shao, H. & Hu, X. *Antheraea pernyi* silk fiber: a potential resource for artificially biospinning spider dragline silk. *J. Biomed. Biotechnol.* **2010**, 683962, doi:10.1155/2010/683962 (2010).
47. Jain, N. K. & Roy, I. Effect of trehalose on protein structure. *Protein Sci.* **18**, 24–36, doi:10.1002/pro.3 (2009).
48. Vollrath, F. & Porter, D. Silks as ancient models for modern polymers. *Polymer* **50**, 5623–5632, doi:10.1016/j.polymer.2009.09.068 (2009).
49. Dicko, C., Knight, D., Kenney, J. M. & Vollrath, F. Conformational polymorphism, stability and aggregation in spider dragline silks proteins. *Int. J. Biol. Macromol.* **36**, 215–224, doi:10.1016/j.ijbiomac.2005.06.004 (2005).
50. Harvey, P. H. & Pagel, M. D. *The comparative method in evolutionary biology*. Oxford University Press, Oxford (1991).
51. Steinberg, T. H., Jones, L. J., Haugland, R. P. & Singer, V. L. SYPRO Orange and SYPRO Red protein gel stains: One-step fluorescent staining of denaturing gels for detection of nanogram levels of protein. *Anal. Biochem.* **239**, 223–237, doi:10.1006/abio.1996.0319 (1996).
52. Reichardt, C. R. C. *Solvents and solvent effects in organic chemistry*. (VCH, Weinheim, 1988).
53. Touchkine, A., Kraynov, V. & Hahn, K. Solvent-sensitive dyes to report protein conformational changes in living cells. *J. Am. Chem. Soc.* **125**, 4132–4145, doi:10.1021/ja0290882 (2003).
54. Ory, J. J. & Banaszak, L. J. Studies of the ligand binding reaction of adipocyte lipid binding protein using the fluorescent probe 1,8-anilinonaphthalene-8-sulfonate. *Biophys. J.* **77**, 1107–1116 (1999).
55. Porter, D. & Vollrath, F. Water mobility, denaturation and the glass transition in proteins. *Biochim. Biophys. Acta* **1824**, 785–791 (2012).

## Acknowledgments

We thank the United States Air Force Office of Scientific Research (FA9550-09-1-0111), the European Research Council (SP2-GA-2008-233409), Magdalen College Oxford, the UK EPSRC (EP/K005693/1; EP/G068224/1) and the Canadian NSERC (PGS 3D/6799-379132-2009) for funding, and our editor at NSR for much appreciated comments and guidance.

## Author contributions

F.V. devised the technology, designed the experiments and wrote the manuscript. N.H. did many of the measurements. D.P., C.H. and M.B.A. discussed the concept and findings with F.V. as well co-analysing the experiments and reviewing the various drafts. M.B.A. finalised all figures. All authors reviewed the manuscript.

## Additional information

**Supplementary information** accompanies this paper at <http://www.nature.com/scientificreports>

**Competing financial interests:** The authors declare no competing financial interests.

**How to cite this article:** Vollrath, F., Hawkins, N., Porter, D., Holland, C. & Boulet-Audet, M. Differential Scanning Fluorimetry provides high throughput data on silk protein transitions. *Sci. Rep.* **4**, 5625; DOI:10.1038/srep05625 (2014).



This work is licensed under a Creative Commons Attribution-NonCommercial-ShareAlike 4.0 International License. The images or other third party material in this article are included in the article's Creative Commons license, unless indicated otherwise in the credit line; if the material is not included under the Creative Commons license, users will need to obtain permission from the license holder in order to reproduce the material. To view a copy of this license, visit <http://creativecommons.org/licenses/by-nc-sa/4.0/>